16 Disordered and Biological Soft Matter

M. Ackermann, C.M. Aegerter, D. Assmann (till January 2015), F. Atzeni (since September 2014), D. Dreher (since July 2014), D. Eder, G. Ghielmetti (till June 2014), A. Keller (since November 2014), F. Lanfranconi, A. Mallavalli (since June 2014), A. Pataki (Master student), S. Puri, L. Schertel (Master student), J. Schneider (since December 2014), L. Selvaggi (since August 2014) and S. Urdy (since July 2014)

in collaboration with: Institute of Molecular Life Sciences (K. Basler, T. Aegerter-Wilmsen, S. Luschnig, L. Pelkmans, D. Brunner), ETH Zürich (P. Koumoutsakos), MPI für Planzenforschung Köln (R.S. Smith), University of Fribourg (A. Jazwinska), University of Bern (C. Kulemeier, S. Robinson, P. Barbier de Reuille), Biozentrum Basel (M. Affolter), University of Strasbourg (N. Rivier), University of Konstanz (G. Aubry, G. Maret, T. Sperling), MPI für Selbstorganisation Göttingen (C.C. Maass), Deutsches Luft- und Raumfahrtzentrum (M. Sperl), University of Twente (A. Mosk), Université Joseph Fourier Grenoble (S. Skipetrov), Université Paris Denis Diderot (F. Graner), Technion Haifa (E. Akkermans).

The group of Disordered and Biological Soft Matter works at the interface of condensed matter physics and developmental biology. The systems of interest are out-of-equilibrium and also address transport in disordered systems. In particular, we are studying the effects of elastic properties and mechanical forces on biological development, including growth and the formation of structures, such as folds in tissues. In disordered media, we are particularly interested in light transport in turbid, multiple scattering samples. We address both fundamental questions, such as the transition to Anderson localization in three dimensions, and applications in imaging techniques relevant for studies of developmental processes in turbid tissues. Finally, we are studying physical models for disordered out-of-equilibrium structures, such as foams. In particular, we are studying foams under diamagnetic levitation, such that distortions due to gravity, which usually mask several interesting non-equilibrium processes, can be eliminated.

Last year, we made considerable progress in several of these areas. Below we focus on Anderson localization, visco-elastic properties of biological tissues and the dynamics of aging, levitated foams.

16.1 Anderson localization of light

Our recent observation of localization of light in highly turbid media [1–3] shows a transition with turbidity as expected from Anderson localization [4, 5]. These results were achieved in TiO_2 samples, which also exhibit a non-linear optical response [6, 7]. The phenomenon is observed in time-resolved experiments through an enhancement at long times when increasing the incoming intensity, see Fig. 16.1. In addition to this intensity dependent increase, there is however also a strongly turbidity dependent increase, combined with a saturation of the width of the photon distribution at long time and therefore localization of

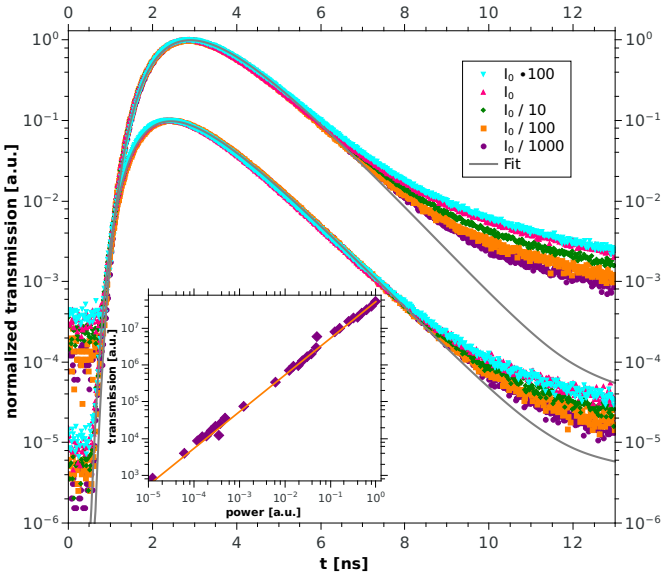

FIG. 16.1 – Characterization of the non-linear response of multiple scattering TiO_2 samples, as given by the power dependence of the time dependent and integrated (inset) optical transmission. The inset shows the transmitted power as a function of input power for a sample with $k \cdot l^* = 2.7$. The time dependent transmission of this sample is shown in the top set of curves for different incident intensities, with $I_0 \simeq 1$ GW/m^2. The bottom set of curves shows a different sample with $k \cdot l^* = 5.7$. This shows that non-linear effects are important only at long times and are not discernible in the integrated transmission.The continuous lines are fits to the analytic solution to the diffusion equation for a slab. As can be seen, at high turbidity, the deviations from diffusive behavior at long times are much enhanced.

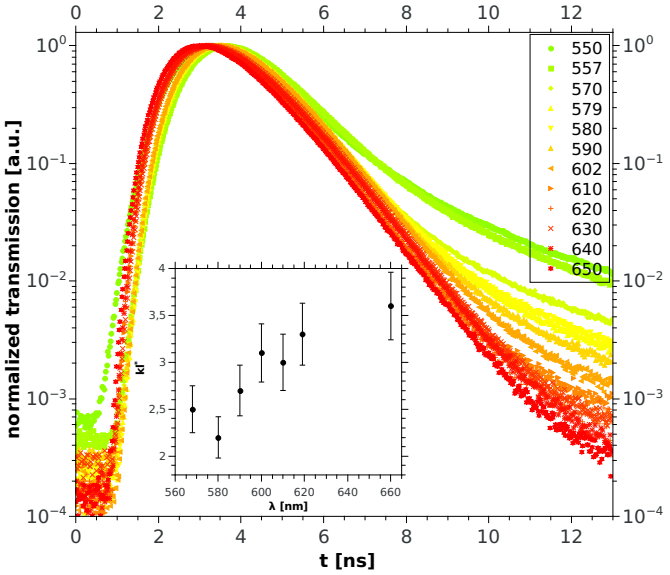

FIG. 16.2 –
Wavelength dependence of the time dependent transmission. As the incoming wavelength is increased, the value of k·l* increases as well (see inset). This means that a scan in wavelength allows for a study of the turbidity dependence of the time dependent transmission. As can be seen by the curves in the main figure, the deviations at long times increase strongly with decreasing k·l*, as expected from a transition to Anderson localization.

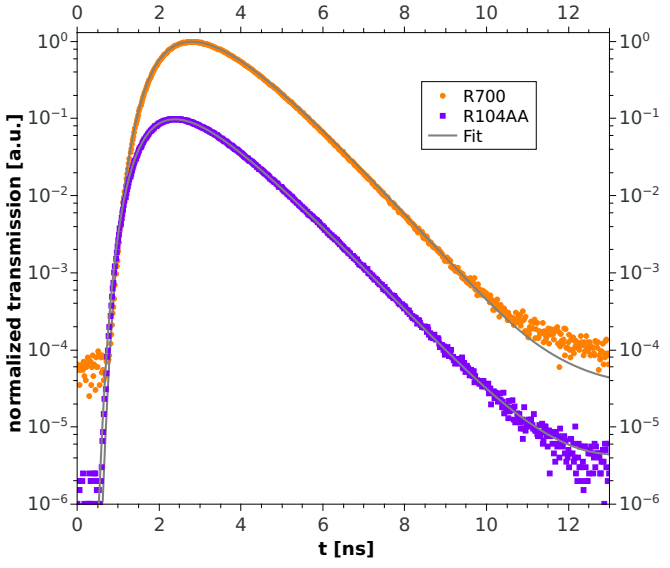

FIG. 16.3 –
Time of flight measurement of a sample with k·l* = 2.7 (orange) and k·l* = 5.7 (purple). In order to check for the influence of wave-length shifts in the outgoing signal, a band pass filter centered around the incoming wavelength (590 nm) was placed behind the sample. Thus these data show the purely elastically scattered part of the light. As can be seen, deviations from diffusion (continuous line) are observed for the sample with k·l* = 2.7.

light. The disentanglement of these two effects allows for an experimental study of the interplay between nonlinearities and localization which we have started in this year [8]. The topic receives increasing interest from theory as well [9–11].

When studying the transition to Anderson localization in three dimensions, it is important to characterize the transition as a function of turbidity and thus separate effects that are due to materials properties and effects due to localization. We achieve this by varying the wavelength of the incoming light, which in turn changes the scattering cross-section and hence the turbidity. Thus, as shown in Fig. 16.2, we can tune the value of k·l*, where k is the wavenumber and l* is the transport mean free path. In addition, we can study the effects of the non-linear processes resulting in a wave-length shift of the outgoing photons due to e.g. mixing and second harmonic effects. Therefore, to study the transition in the elastic component, we are using band pass filters centered around the incoming wave-length, positioned behind the sample. This way, it is still possible to observe long-time deviations from diffusive behavior appearing with increasing turbidity, as expected from localization, see Fig. 16.3. In addition, the increase in the non-linear, frequency shifted component with increasing turbidity can be used to gain information about the intensity distributions of the localized modes. The strong increase in this part of the signal indicates a highly skewed intensity distribution in the sample, as predicted theoretically [12], which we would not be able to discern in these samples otherwise due to temporal fluctuations in the signal averaging out the speckle pattern.

[1] M. Störzer, P. Gross, C.M. Aegerter and G. Maret, Phys. Rev. Lett. **96**, 063904 (2006).

[2] C.M. Aegerter M. Störzer, and G. Maret, Europhys. Lett. **75**, 562 (2006).

[3] T. Sperling, W. Bührer, C.M. Aegerter, and G. Maret, Nature Photonics **7**, 48 (2013).

[4] P.W. Anderson, Phys. Rev. **109**, 5 (1958).

[5] E. Abrahams *et al.*, Phys. Rev. Lett. **42**, 673 (1979).

[6] R.Adair, L.L.Chase and S.A.Payne, Phys.Rev.B, **39**, 3337 (1989).

[7] C.C. Evans *et al.*, Optics Express **21** 18582 (2013).

[8] T. Sperling, W. Bührer, M. Ackermann, C.M. Aegerter, and G. Maret, New J. of Phys. **16**, 112001 (2014).

[9] C.Conti, Chin.Phys.Lett. **31** 030501 (2014).

[10] S. Fishman, Y. Krivolapov, and A. Soffer, Nonlinearity **25** R53 (2012).

[11] N. Cherroret, B. Vermersch, J.C. Garreau, and D. Delande, Phys. Rev. Lett. **112**, 170603 (2014).

[12] T.M. Nieuwenhuizen and M.C. van Rossum, Phys.Rev.Lett. **74**, 2674 (1995).

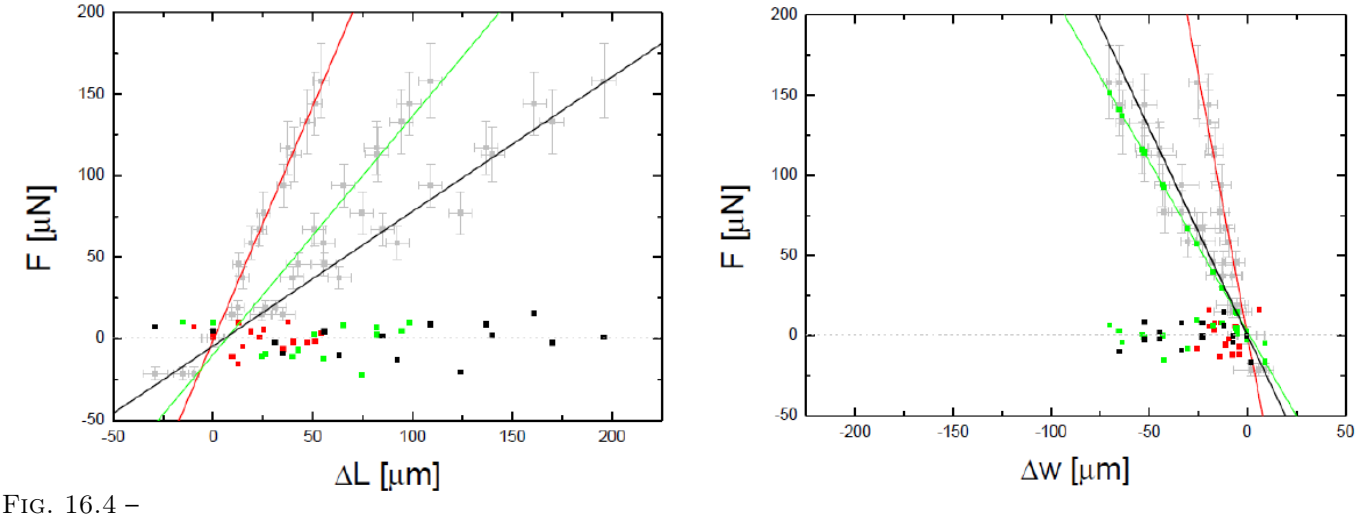

FIG. 16.4 –
Force-extension curves for a wing disc. The left panel shows the length of the disc in the direction of pulling, the right one the width perpendicular to this direction. The curves represent linear fits to different parts of the wing disc (pouch: red, hinge-notum: green, total disc: black). Raw data are grey and the coloured symbols are the residuals of the fits. Even for large deformations the wing discs are surprisingly linear in their elastic behaviour. From a study of the lateral constriction and the extension we find a Poisson ratio very close to 0.5.

16.2 Visco-elastic properties of Drosophila wing disc

In the course of our investigations into the influence of mechanical force on growth regulation in the wing imaginal disc of Drosophila [1–6], we are also studying the visco-elastic properties of this tissue directly using force-extension measurements [7, 8]. For this purpose, we have built a mechanical forcing stage capable of applying forces in the range of 10 to 500 μN onto the tissue in a temporally varying manner [7]. As can be seen in Fig. 16.4, the mechanical response of the tissue is linear over a very large range of extensions and different parts of the tissue show extensions relative to their lengths, corresponding to a uniform Young's modulus over the whole tissue. This is irrespective of the fact that these different parts of the tissue are developmentally distinct and lead to different structures in the adult fly.

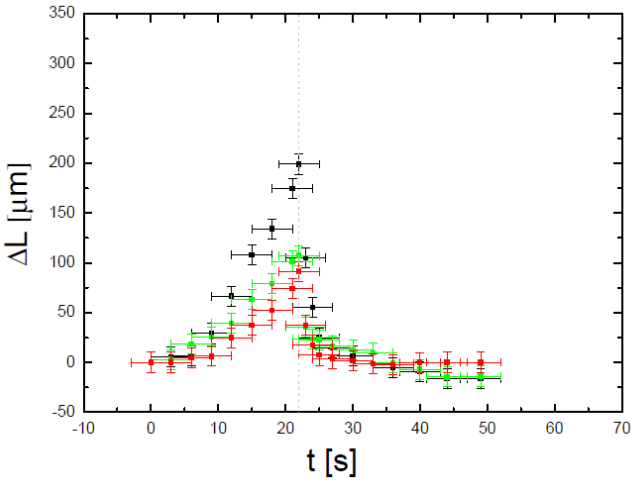

FIG. 16.5 – Determination of the visco-elastic behavior of a wing-disc tissue. When released from tension (dashed vertical line), the wing disc relaxes to the un-stretched state on a time scale of several seconds. Similarly, a temporally increasing force is delayed in the straining of the tissue. This fits well with the description of the tissue as a Kelvin-Voigt material with a high internal viscosity.

Applying a temporally varying force (linearly increasing until a sudden release), we can study the viscous properties of the tissue as well. An example is shown in Fig. 16.5, where the observed mean time of force application and release is τ = 12(3) s. This behavior is well described by a Kelvin-Voigt model of the tissue with a Young's modulus of E = 80(15) kPa and a viscosity of η = 1.0(3) MPa · s. The results imply that the tissue is insensitive to mechanical stress on time scales shorter than τ, as are for instance incurred due to larval motion [8].

[1] T. Aegerter-Wilmsen, C.M. Aegerter, E. Hafen, and K. Basler, Mechanisms of Development **124**, 318 (2007).

[2] U. Nienhaus, T. Aegerter-Wilmsen, and C.M. Aegerter, Mechanisms of Development **126**, 942 (2009).

[3] U. Nienhaus, T. Aegerter-Wilmsen, and C.M. Aegerter, PLoS One **7**, e47594 (2012).

[4] T. Aegerter-Wilmsen *et al.*, Development **137**, 499 (2010).

[5] T. Schluck, U. Nienhaus, T. Aegerter-Wilmsen, and C.M. Aegerter, PLoS One **8**, e76171 (2013).

[6] T. Aegerter-Wilmsen *et al.*, Development **139** 3221 (2012).

[7] T. Schluck and C.M. Aegerter, Eur. Phys. J. E **33**, 111 (2010).

[8] T. Schluck, PhD thesis, University of Zurich (2013).

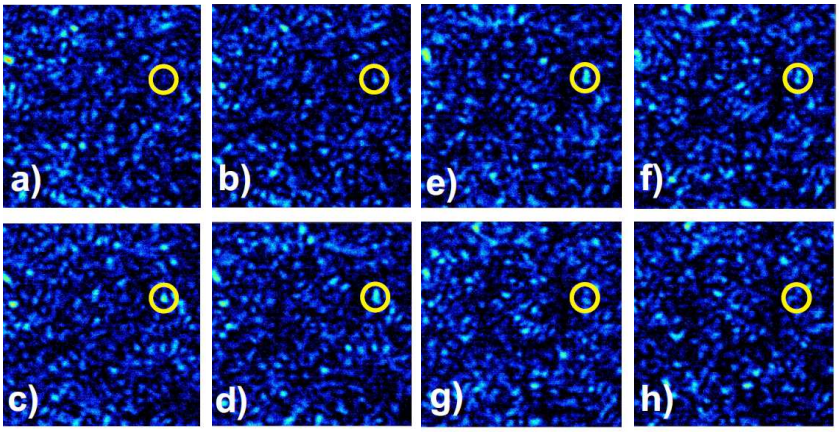

FIG. 16.6 – Time evolution of the speckle pattern of a foam with 20% liquid fraction and an age of about 100 min. The images taken with a movie camera are spaced by 10 ms. The dynamics of the time evolution of the pattern is evidenced by the encircled speckle that comes and goes. From the analysis of all speckles in the images, the correlation time has been obtained as a function of age.

16.3 Dynamics of levitated foams

Using diamagnetic levitation [1–3], we have studied the coarsening behavior of foams of different liquid fractions [4, 5]. While this has been studied theoretically for a long time yielding different predictions for dry foams by von Neumann [6] and wet foams by Ostwald [7], an experimental investigation has proven difficult due to the drainage of liquid by gravity. Given different coarsening dynamics at different liquid fractions according to the predictions [4], we have now studied the microscopic dynamics in the different regimes in more detail. Using diffusing wave spectroscopy [8, 9], i.e. the correlation of speckles in multiply scattered light transmitted through the foam (see Fig. 16.6), we determine the correlation time of the speckle, thus characterizing the dynamics of the scatterers in the foam. Doing this for several speckles at once using a high speed camera, allows us to study the time dependence of this dynamics on several time scales:

- the time scale of the scatterer movements themselves, which corresponds to the correlation time
- the time scale of the age of the foam, which determines the coarsening behaviour and therefore influences the dynamics of the scatterers
- the intermediate time scale on which the foam as a whole shows movements, resulting in strong fluctuations in the correlation time.

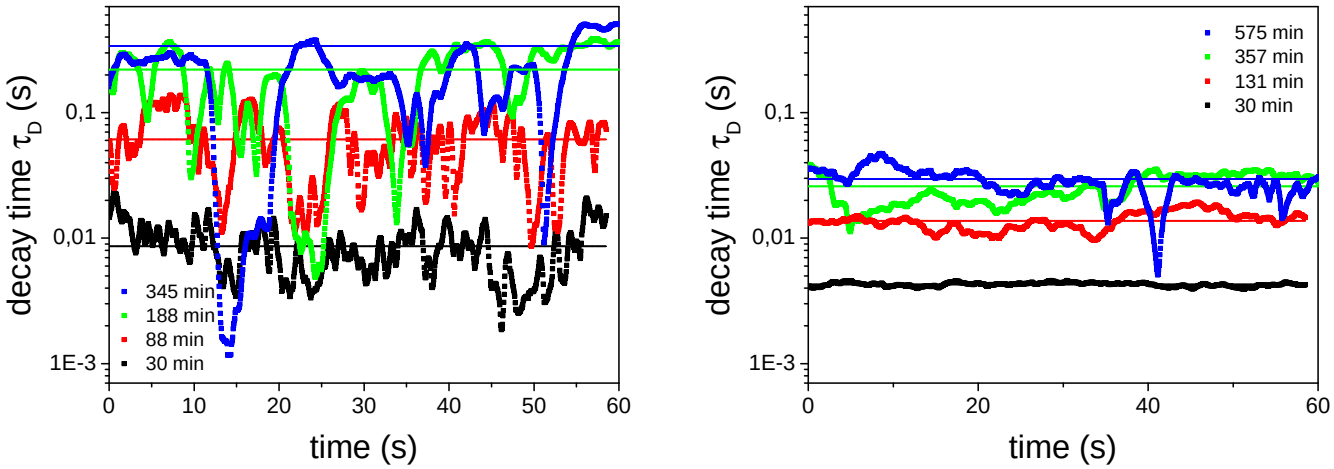

FIG. 16.7 – Time evolution of the DWS decay time as determined from speckle patterns as in Fig 16.6 for two different liquid fractions (left: 19%, right 34 %) for varying ages. Apart from an overall increase of the average decay time caused by the coarsening of the foam, a marked change in the dynamics is seen for the dry foam. At higher age, the dynamics is dominated by intermittent bursts of activity corresponding to large scale rearrangements of bubbles, which become less frequent as the foam coarsens. In wet foams in contrast, the dynamics is not dominated by single events, but rather by random fluctuations. In addition, the time scale of the decay time is much faster, connected to the ballistic motion of bubbles between collisions.

Figure 16.7 indeed shows striking differences in observed dynamics between foams of different liquid fractions [5]. At low liquid fraction, where the bubbles are strongly connected, there are intermittent large bursts of activity, corresponding to macroscopic rearrangements of the bubbles. The frequency of these bursts decreases with age as the foam coarsens according to the predictions of von Neumann [5, 6]. At high liquid fractions, where bubbles are separated from each other, there are no bursts of activity and dynamics does not change greatly with the age of the foam, apart from the change in time scale due to the increase in bubble size. Similarly, the coarsening process is not homogeneous in time, but is described by van Neumanns law at long times, when the larger bubbles start to overlap and by Ostwald ripening at short times, see Fig. 16.8.

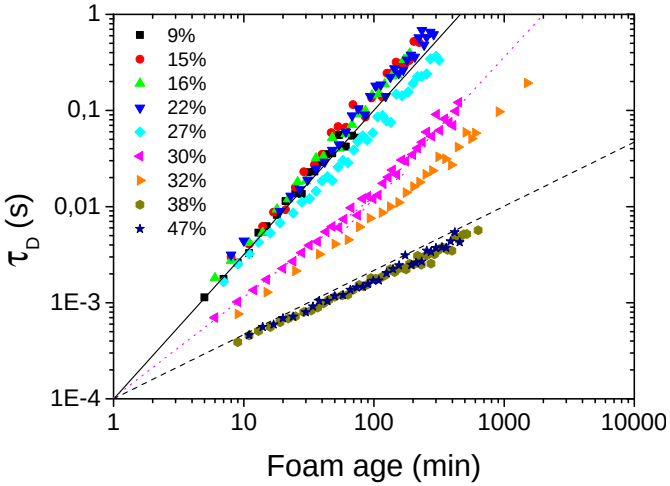

FIG. 16.8 – DWS correlation times obtained from integrating g_2 for several foams as a function of foam age. At low liquid fraction, the correlation time scales with age3/2(full line), whereas at high liquid fraction it scales as age2/3(dashed line). Around liquid fractions of 30%, close to the transition, two regimes corresponding to the limiting cases can be seen.

[1] W. Braunbeck, Z. Phys. **112**, 764 (1939).

[2] M.V. Berry and A.K. Geim, Europ. J. Phys. **18**, 307 (1997).

[3] C.C. Maass, N. Isert. G. Maret and C.M. Aegerter, Phys. Rev. Lett. **100**, 248001 (2008).

[4] N. Isert, G. Maret, C.M. Aegerter, Europ. Phys. J. E **36**, 116 (2013).

[5] N. Isert, G. Maret, C.M. Aegerter, Colloids and Surfaces A **473**, 40 (2015).

[6] J. von Neumann, in *Metal Interfaces* (C. Herring ed.), 108 (1952).

[7] W. Ostwald, Z. Phys. Chem. **37**, 385 (1901).

[8] G. Maret and P.E. Wolf, Z. Phys. B **65**, 409 (1987).

[9] D.J. Pine, D.A. Weitz, J.X. Zhu and E. Herbolzheimer, J. Phys. **51**, 2101 (1990).